

Real sandpiles: dilatancy, hysteresis and cooperative dynamics

Anita Mehta

IRC in Materials, University of Birmingham, Edgbaston, Birmingham B15 2TT, UK

The microscopic dynamics of real sandpiles forms the focus of this article, with particular reference to dilatancy and hysteresis, which are of fundamental importance in the characterisation of granular systems. The competition and cooperation between independent-particle and collective excitations is examined using novel theoretical and computational techniques. These methods yield a wealth of detail on the microscopic structure of granular flows, as well as on the static configurations that these generate.

1. Introduction

Although granular materials have been studied by engineers [1] for a long time, it is only recently in their reincarnation as “sandpiles” that they have become a fashionable and exciting area of theoretical [2–10] and experimental [11–14] physics. Despite our childhood experiences with them, the physics of sandpiles is very complicated, and it is worth asking ourselves why this is. The answer is that they combine some of the most complex aspects that are known in physical systems. In addition to phenomena exhibited by other amorphous systems, their randomness of shape and texture strongly influences their static and dynamic properties. Sandpiles are highly nonlinear and hysteretic, as a consequence of which they show complexity, so that the occurrence and relative stability of a large number of metastable configurations govern their behaviour. They exhibit behaviour that is neither completely solid-like nor completely liquid-like, but which is intermediate between the two. Like liquids, powders can take the shape of their containing vessel, but unlike them, they can also adopt a variety of shapes when they are free-standing. This leads to the everyday phenomenon of the angle of repose, which is the angle that a sandpile makes with the horizontal. In reality, the angle of repose is not unique, but depends on the history of the sandpile: this is related to, among other things, the phenomenon of dilatancy [16], which is the ability of granular materials to sustain different degrees of packing.

Although the microscopic physics of granular materials is in its infancy, there

has been a long tradition of interest in this field by eminent physicists such as Coulomb [15], who estimated the maximum angle of repose in terms of a phenomenological coefficient of friction, and Reynolds [16], who studied dilatancy. One of the modern fathers of the field was Bagnold, who did pioneering theoretical and experimental work on relating angles of repose after shear to the so-called Bagnold angle of dilatancy [17]. A valuable handbook describing some of this work and containing a large number of experimental results was written by Brown and Richards [18]. All of this work was at a macroscopic level, and is invaluable because it provides critical tests for realistic microscopic theories being developed at present [2, 9, 19, 20].

Because the understanding of sandpiles presents such an enormous challenge, there have been a plethora of different approaches, which have sought to tackle one difficulty at a time. For instance the continuum approaches of Haff [21] and others and the hydrodynamic approaches of Jackson [22] are valid in the regime of rapid shear (the so-called grain-inertial regime) where the concept of an effective granular temperature based on the root-mean-square velocities of particles is used. These methods are, however, inappropriate for the situation where the grains are in slow, or no, motion with respect to each other – the continuum approach fails, because the discreteness of the grains and the effects of friction and restitution at individual collisions become increasingly important. In our work [2, 4, 5, 6, 9, 10] we have concentrated on the opposite regime of slow shear (the viscous regime), where the discreteness of the particles is important because they stay in contact with one another for longer. In particular we have looked at the statistical mechanics of powders, which formulates an alternative concept of an effective temperature called compactivity (this is related to the packing and is also valid [3–5] for particles at rest); the focus of our work, however, has been the microscopic dynamics of sandpiles. These issues are beset with great difficulties; however, the strength of our approach is that we have always tried to incorporate the classical phenomena of hysteresis, dilatancy, discreteness of particles and disorder. Our deep-seated convictions about the physics underlying sandpile dynamics set this approach apart from recent theories of self-organised criticality (SOC) [23], which claim to describe sandpiles: we will discuss them in a later section.

2. A brief digression on sandpiles at rest

Although the main focus of this article is sandpiles in motion, it is appropriate to review briefly what is known about sandpiles at rest. The statistical mechanical theory of powders, first put forward by Edwards [3], has been applied [4] to problems of packing: its starting point is the “ergodic

hypothesis” of powders – all powders with the same specification of contents, formed by *extensive manipulation* (by which we mean processes of stirring, pouring, shaking, etc., which do not act on individual grains) and *occupying the same volume* have the same macroscopic properties. It is worth emphasising at this stage [2] that the static configuration we study is *the end result of many dynamical processes*, which were responsible for the motion of the powder through its phase space.

The central analogies with conventional statistical mechanics are [2, 3] the following:

Thermal system		Powder
energy, E	\equiv	volume, V
temperature, T	\equiv	compactivity, X

which satisfy corresponding thermodynamic relations. For example, the compactivity X satisfies

$$X = \partial V / \partial S \quad (1)$$

with S as the entropy. The entropy here has dimensions of volume, and can be formulated in terms of disorder induced by voids [2]; for instance, the state of minimum entropy will be that corresponding to random close-packing, where although there is always *geometric* disorder, there is a minimal amount of *void-related* disorder. The interested reader is referred to the appropriate references [2–4] for more details; I will focus here on the physical meaning of the analogies we have drawn. The volume V is that which is actually occupied by the powder, which has a well-defined minimum (random close-packing) and a maximum that is reached when the powder is at most fluffy – the analogy with the energy E as defined in the canonical ensemble for thermal systems, is obvious. The compactivity X (like the temperature T for thermal systems) is a measure of the disorder: when $X = 0$, the powder is *constrained* to be at its most compact, whereas the reverse holds for $X = \infty$. The introduction of the concept of compactivity injects a remarkable degree of universality into the problem, so that the *same* compactivity characterises powders composed of grains of different local sizes, densities and shapes.

The next step is to write down an expression for an equivalent granular “Hamiltonian” W , which gives the total volume V as a function of the positions and coordination numbers of the individual grains. Since powders are amorphous, this is very difficult to do! Although taking a lattice-based approach

might seem to be a drastic approximation, it turns out that it is possible by this means to get valuable insights into the problem of granular packing without obscuring its salient features.

The problem of a binary mixture of spherical grains of radii R_1 and R_2 respectively has been discussed at length elsewhere [2, 4] where it has been mapped onto the Bragg–Williams problem of the A–B alloy. It is possible to write the W -function for this as

$$W = -\frac{1}{2} \sum_{\langle ij \rangle} J \sigma_i \sigma_j, \quad (2)$$

where $\sigma_i = \pm 1$ depending on whether site i is occupied by an A or a B grain, and J is a measure of the relative ease with which grains pack when they are of the same size, as opposed to when they are of different sizes (so that J can be used to model physical effects like cohesion or surface roughness). The solution to this is (within a mean field approach)

$$\langle \sigma \rangle = \tanh(zJ \langle \sigma \rangle / \lambda X) \quad (3)$$

with z the coordination number of the lattice, and λ the analogue of Boltzmann's constant. Thus for $zJ/\lambda X < 1$, the two types of grains are totally miscible, but for $zJ/\lambda X > 1$, they tend to have unequal mixed domains until at $X \rightarrow 0$, the material separates into domains of pure A and pure B. In other words, apart from any natural affinity J for similarly sized grains to be near each other, the other important parameter is the compactivity X , so that if, say, space-saving considerations are important (small X), then the simplest picture is that grains of disparate sizes will segregate in order to achieve this. On the other hand, if the powder is not so constrained, a random mixture of the two species will be the end state of an extensive dynamical process such as shaking or stirring.

However, while total segregation and complete miscibility are extreme cases of what can happen to a powder if we shake it for a long time, the real picture is somewhat more complex; it turns out that the spin representation of the zero-field eight-vertex model [2, 4] is more appropriate, rather than the above Ising-like model. The nature of the “ordered” state *must* depend on the ratio R_1/R_2 . For low R_1/R_2 , when the size of the smaller grain is smaller than the average pore size of an assembly of the larger ones, the former will, on shaking, slip through the holes created by the latter, leading to segregation; for ratios closer to unity, on the other hand, one gets a form of stacking [2, 4]. For intermediate values of R_1/R_2 , the nature of the packing should be some sort of superposition of these two “ordered states” – thus, while many of the smaller

grains segregate, there are some which stack. The results of the eight-vertex model of powders are in qualitative accord with this, as the spin configurations corresponding to segregation and stacking are in that model degenerate: the details are discussed elsewhere [2, 4]. The important point is that the development of this statistical mechanical framework, for all its simplicity and apparent abstraction, provides an excellent basis for the investigation of real properties relevant to the packing of granular materials.

Before leaving the subject of static powders, I would like to raise a few concluding questions:

- It is evident that at extremal values of the ratio R_1/R_2 , the degeneracy between the stacked and segregated solutions will be split. This is equivalent to solving the eight-vertex model in a finite field, a problem which has not been solved analytically: we are [24] trying to look at this computationally to see if the use of spinodal decomposition-type ideas allows us to predict which of the two “ordered” states the system evolves to.

- Many of our predictions [2, 4] are qualitatively valid for concentrated suspensions, which can, for high Péclet number, show behaviour similar to dry powders [25]; we await a closer link between experiment and theory in this area.

- It is possible within the statistical mechanical framework to account for polydispersity by using a Potts-model-type formulation. However, to capture the disorder inherent in sandpiles, one needs to use spin-glass-type W -functions – I hope that experts in spin glasses will soon apply their expertise to formulating and solving appropriate “Hamiltonians” for static powders, which would be the next major breakthrough in the statistical mechanical development of the field.

3. Sandpiles in motion: on the dynamics of relaxation

I have so far discussed the static configurations that result when a powder has undergone some extensive dynamical process: I would now like to discuss what happens *during* such a process, which for me is the more intriguing question. True thermal agitation in a powder takes place on an atomic rather than a particulate scale; therefore it is external vibrations that play an essential role in the behaviour of powders. However, the vibrations can to some extent be discussed in terms of temperature-like quantities. In the absence of external agitation the grains are frozen into one configuration (since their thermal energy is insufficient to generate the equivalent of Brownian motion), which represents one of the many possible *metastable* states of the system (this is one of the reasons why powders show *complexity*).

When mechanical energy is supplied to a powder, in the form of stirring, shaking or conveying operations, periods of release are introduced. During the periods of release the grains have some freedom to rearrange their positions relative to their neighbours and the powder “jumps” [2] between different, but related, grain configurations. In this case a series of grain configurations represents the dynamic response of the powder to forcing excitations. Thus a shaken powder follows a path through the phase space of powder configurations, which depends on both the dynamics of the individual grains and on the intensities and frequencies of the component vibrations of the driving force.

Recently, experimenters [11] at the James Franck Institute in Chicago have examined the relaxational response of a powder to vibration. The phenomenon they study is very simple: they observe the rate of decay of the angle of repose θ of a granular pile submitted to vibration of varying intensities. What they found is that for large intensities of vibration, the slope of the pile decays to zero such that its relaxation is proportional to the logarithm of the time, whereas for smaller intensities, the slope of the pile stays finite (within the time of measurement), and the relaxation appears slower than logarithmic. This motivates the following questions: what happens when a powder is shaken? Can we explain the different relaxation rates seen in the Jaeger et al. experiment [11] by a microscopic model of the physics? What is the effect of shaking on the structure of the powder?

In the next subsection, I will describe the microscopic picture of relaxation that I have formulated [2] to answer these questions: in the ones that follow it, I will discuss the computational [6, 10] and analytical [5, 9] work that we have done in order to test this picture.

3.1. Microscopic picture of granular relaxation

Let us divide up the free surface of a granular pile into a collection of local clusters (fig. 1), and then model each cluster as a multi-particle potential well [2], so that particles in the latter are ordered in terms of their stability. The equivalence is made as follows: surface particles that are closely packed such that each particle is stable, form a *locally* stable cluster, and can be represented (cf. cluster I in fig. 1b) by an equivalent potential well where the corresponding particles are at the bottom of the well, i.e. have low potential energies. Conversely, when there are voids (cf. cluster II in fig. 1b), the surface particles are loosely packed and the cluster is *unstable to small vibrations*; the equivalent potential well has particles that have high potential energies. It is perhaps worth making explicit here that these wells are of variable depth (where the depth of a well depends on the local slope and the height up the pile of the corresponding cluster) so that the barriers between neighbouring wells are also

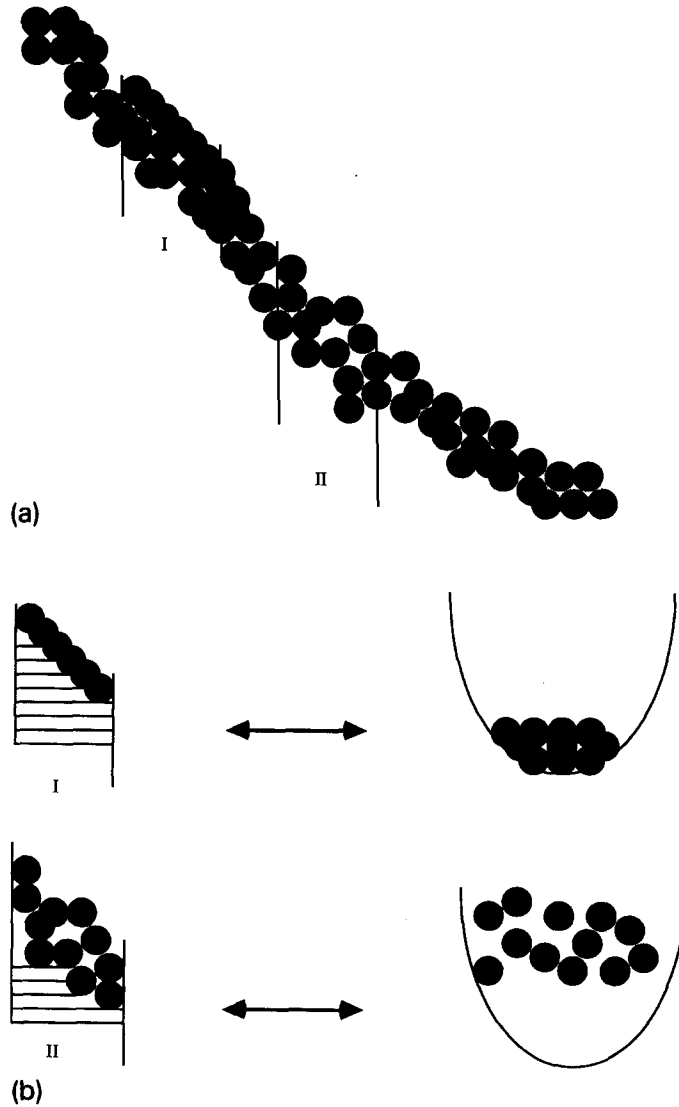


Fig. 1. (a) The surface of a sandpile: this is divided up into local clusters, of which clusters I and II are examples. (b) The equivalent potential wells of clusters I and II; note that these wells exist in potential energy landscapes, so that the ordering in the wells is in terms of energy, rather than position. This is emphasised by drawing disjoint grains for the equivalent well in cluster II.

of variable height. Clearly the criterion of global stability of the pile imposes inter-well and intra-well interactions on this picture, so that if one particle is ejected from its well, it will change the landscape of its own well in addition to that of the one in which it lands.

The effect of vibration applied to the pile is modelled [2, 6, 9, 10] as being a noise H acting on this assembly of wells. If H is greater than the binding energy of the particles to their wells, then the particles are ejected, and move into neighbouring wells: in terms of the real surface, this means that particles are ejected individually (*independent-particle relaxation*) from their clusters and travel down the pile. Conversely, if H is small relative to the binding energies of the particles, they are not ejected: this energy is, however, not lost to the system, because the particles reorganise collectively (*collective relaxation*) within their wells to minimise voids. The claim is [2, 6, 9, 10] that for high intensities of vibration, the dominant process is independent-particle relaxation at the surface leading to avalanches down the slope, whereas collective relaxation dominates at low intensities.

What are the consequences of this model? Let us remind ourselves that independent-particle relaxation leads to a rapid decay of the slope, since overhanging particles are constantly being displaced; but since the cascading particles are in tumult, as it were, this process will not lead to the most efficient packing, or to the lowest compactivity. Equally, we would expect that when collective relaxation dominates, the slope will relax slowly or not at all, but the slow collective reorganisation of particles will lead to efficient void-filling, i.e. to low compactivities. Thus in terms of the experimental results [11], we would expect the faster decay of the slope to be accomplished by predominantly independent-particle relaxation and to result in high compactivities (low densities). On the other hand, for small intensities of vibration, we would expect to see a pile of finite (non-zero) slope, relaxing slowly via clusters of particles reorganising collectively to lead to a much denser packing (low X).

These expectations are borne out by computational and analytic work, which I will describe in the next subsections.

3.2. Computer simulation approaches

We have investigated the structure and dynamics of powders submitted to vibration by non-sequential and cooperative computer simulation approaches in two and three dimensions. In the two-dimensional work [6], we looked at the decay of the slope of a sandpile subjected to vibration, while in the three-dimensional work [10], we analysed the effects of the relaxational dynamics on the structure of the powder and the correlations within it.

For a non-cohesive powder, it is clear that stirring, shaking and pouring are all many-particle operations. During these processes the particles follow complicated trajectories, composed of free fall segments punctuated by hard, inelastic collisions with the other particles before they all reach stable positions in a static assembly. These are fundamentally non-sequential, that is, the route

of one particle to its stable position cannot be computed without simultaneously computing the routes of many other particles. Stable configurations are those in which each particle rests in a potential energy minimum, and therefore cannot lower its potential energy any further by local *or* non-local motion. In practice (in three dimensions), this means that each particle is in contact with at least three others.

The static configurations of grains which result from shaking reflect the essentially non-sequential nature of the process. These configurations contain particle bridges [6, 10] and a wide variety of void shapes and sizes which do not occur in sequentially deposited aggregates. In this context a bridge is a stable arrangement of particles in which at least two of the particles depend on each other for their stability. Bridges cannot be formed by the sequential placement of particles into stable positions but are a natural consequence of the simultaneous settling motion of closely neighbouring particles. In our simulations [6, 10] we have approximated the precise particle trajectories by using a low-temperature Monte Carlo method supplemented by a non-sequential random close packing algorithm. This is a compromise. At the expense of losing information concerning the granular dynamics we can efficiently produce static structures which correspond to a non-sequential deposition process. Previous simulations [26–29] have failed to build in this aspect of shaking.

3.2.1. Review of other work

It is pertinent, at this point, to give a brief survey of reorganisation schemes, in order to explain the philosophy underlying our own. Since the static powder is only characteristic of the method of preparation, an ensemble of configurations, built from independent realisations of the whole powder using the same method, is representative of a particular aggregation method. Many aggregation schemes have been investigated in this way including the deposition model of Vold [26], ballistic deposition [27], close-packing with surface restructuring [28] and diffusion-limited aggregation [29]. Of these schemes, the simplest is the Vold model, in which particles stick instantaneously on impact. In ballistic deposition, no trajectories are computed, and aggregation sites are chosen from a list, while in diffusion-limited aggregation, random walk trajectories precede the aggregation phase. In all these cases, the initial choice of a site terminates the process, i.e. particles stick on impact. The model of ref. [28] goes further, in that particles are allowed to roll around after impact on a *stationary* aggregate, until they find a local minimum of potential energy – but this is *still* a sequential process. In contrast, the schemes that we have developed [6, 10] contain collective restructuring – where the aggregate restructures simultaneously with the incoming particles – thus making our process

non-sequential and cooperative, and therefore capable of incorporating realistic reorganisation processes. This essential ingredient makes our methods much more reflective of many-particle events in a moving granular system.

As well as our own, there are a couple of other non-sequential schemes around in the literature: the well-publicised “Brazil nut” scheme of Rosato et al. [30] was built around a two-dimensional non-sequential Monte Carlo method to study the size segregation which is induced by shaking. However, it does not include a criterion for the stability of the packing and hence cannot be used, directly, to follow the changes in volume fraction or particle coordinations which occur as a result of applied vibrations. (In fact, its conclusions about larger particles rising to the top have been well known for a very long time – the work of Bridgwater [1] in particular describes in great detail the effect of physical constraints in determining the size segregation behaviour, and indeed the phenomenon of large particles rising to the top is by no means universal!) In a three-dimensional simulation, Soppe [31] produced non-sequential consolidated packings by combining a Monte Carlo compression with ballistic deposition. This method also omits an explicit stability criterion and, by using a particular prescription for annealing the packing, it leads to unstable beds of particles with volume fractions $\phi = 0.60$.

Cellular automata [21] are being used increasingly to model granular flow; while these are powerful tools both because of their flexibility and their relative speed, they are limited by their lattice-based formulation. They may be used for qualitative descriptions of powder flow, but cannot probe detailed particulate structure during and after flow. Simulations of powders have also been done using granular dynamics, which are usually performed in one of two distinct regimes. Firstly there is a grain-inertial regime [32,33] in which instantaneous, inelastic two-particle collisions dominate the motion. These simulations model powders under highly energetic (kinetic) flow conditions and they are most efficient at moderate particle densities of $\phi \cong 0.3\text{--}0.4$. In many ways the implementation of granular dynamics in the grain-inertial regime follows the standard methods established for the molecular dynamics of complex fluids using collections of rough hard spheres. However, one important distinction arises because the collisions between particles, unlike those between molecules, are inelastic. The second granular dynamics regime, called the quasi-static regime, is used to model [34] the slow, collective motion of close-packed ($\phi \cong 0.55$) collections of particles. In this case the contact forces between two particles are most important and the organization of computer simulations revolves around the efficient solution of many simultaneous equations of motion for interacting particles. For most real materials the precise nature of the contact forces is unclear; the so-called principles of limiting friction and indeterminacy of stress [18], which are familiar to chemical

engineers [1], say that the internal stress in a granular assembly is indeterminate, because the friction between two grains in contact can lie anywhere between zero and a limiting value. Therefore the applications of granular dynamics in the quasi-static regime [34] are restricted by (ad hoc) estimates of contact forces usually constructed from viscous and harmonic elements.

All of this emphasises the need for a different kind of approach, which is discussed below.

3.2.2. *Details of our method and results*

Most shaking processes take place in a series of regimes which traverse the spectrum from grain-inertial to quasi-static and therefore “shaking” is difficult to simulate with a continuously tuned granular dynamics prescription. Thus during a cycle of a shaking process, the grains may experience local particle densities which vary from $\phi \approx 0.3$ – 0.6 and may go through periods of rapid motion as well as through periods of slow relaxation. Our method [6, 10] is able to probe details of particulate structure since it falls between authentic granular dynamics simulations [32, 33] and previous shaking simulations [27], which combine sequential deposition with a search for global minima of the potential energy. Since, in addition, we do not assume a continuum basis or a single granular temperature, we are able to cope better with the quasi-static regime of slow shear.

Our aim is to distinguish, in terms of individual and collective relaxations [2], the different microscopic responses which underlie the macroscopic response of a powder subject to vertical vibrations at different intensities. In our simulation model [6, 10] the driving force is periodic, and leads to clearly defined periods of dilation of the powder assembly, between which we have static configurations of grains. The driving force is applied uniaxially and is coupled homogeneously to the powder so that free volume is introduced uniformly. During the periods of dilation the grain motion is dominated by a strong uniaxial gravitational field and by hard-core interactions with neighbouring particles and the container base.

In our simulations [6, 10] we have a bed of monodisperse, hard spheres above a hard, impenetrable, plane base which is at $z = 0$. The particle bed is periodic, with a repeat distance of L sphere diameters, in two perpendicular directions, x and y , in the plane. Each primary simulation cell contains N spheres. A unidirectional gravitational field acts downwards, i.e. along the negative z -direction.

Initially the spheres are placed in the cell using a sequential random close-packing procedure [35]. The spheres are introduced, one at a time, from large z and at random lateral positions, and follow complex paths, which are

composed of vertical line segments and circular arcs, until they reach stable positions in contact either with three other spheres or with the hard base. These sphere trajectories correspond to rolling motions separated by periods of free fall. In this sequential deposition, the moving sphere rolls over spheres that are already located in stable positions; that is, incoming spheres cannot disrupt the stable packing and they cannot interfere with other aggregating particles. In this sense the aggregation is slow and the gravitational field is strong. Many authors have analysed the sequential, close-packed arrangements of spheres [27, 36, 37] which are obtained using this procedure. For monodisperse spheres there are boundary layers which extend for approximately five sphere diameters both above the hard base and below the free surface. These layers contain quasi-ordered arrangements of spheres. Apart from this, the packing is homogeneous with a mean volume fraction, $\phi_0 = 0.581 \pm 0.001$, and a mean sphere coordination $c_0 = 6.00 \pm 0.02$ [38]. These values are not altered substantially by introducing a small amount ($\sim 5\%$) of polydispersity and they adequately describe the packings which are used as initial configurations for our shaking simulations.

In our simulations the packing is subject to a series of non-sequential, N -particle reorganisations. Each reorganisation is performed in three distinct parts: firstly a vertical expansion or dilation, secondly a Monte Carlo consolidation, and finally a non-sequential close-packing procedure. We shall call each full reorganisation a shake cycle or, simply, a shake. The duration of our model shaking processes, and the lengths of other time intervals, are conveniently measured in units of the shake cycle.

The first part of the shake cycle [6, 10] is a uniform vertical expansion of the sphere packing, accompanied by random, horizontal, shifts of the sphere positions. In the second phase of the cycle the whole system is compressed by a series of displacements of individual spheres. Spheres are chosen at random and displaced according to a very low temperature, hard sphere, Monte Carlo algorithm. Finally the sphere packing is stabilised using an extension of the random close-packing method described above. The spheres are chosen in order of increasing height and, in turn, are allowed to roll and fall into stable positions. In this part of the shake cycle spheres may roll over, and rest on, any other sphere in the assembly. This includes those spheres which are still to be stabilised and which may, in turn, undergo further rolls and falls. In this way touching particles can be continually moved until no further rolling is possible. This procedure allows the formation of complex, stable, structural components, like bridges and arches, which *cannot* be constructed by purely sequential processes [6, 10].

The outcome of a shake cycle is to replace one stable close-packed configuration by another. In these configurations each particle forms part of a cluster

that includes its neighbours, and a “shake” is thus a reorganisation scheme for a set of clusters. The role of the individual parts of the shake cycle is clear. Expansion represents a challenge of variable degree to the integrity of the clusters. The Monte Carlo compression reinstates those clusters that were deformed and, when necessary, creates new clusters where the previous ones were destroyed. Finally the stabilisation phase positions the particles inside the set of clusters established in phase two.

In practice during phase one of the n th shake cycle the mean volume fraction of the assembly falls from ϕ_{n-1} to $\phi_{n-1}/(1 + \epsilon)$. In phase two the volume fraction steadily increases to $\phi_n \cong \phi_{n-1}$ and in phase three it remains approximately constant. In contrast the mean coordination number is reduced from c_{n-1} to zero in the expansion phase of the n th shake and remains zero throughout the Monte Carlo compression but, during stabilisation, it increases steadily to $c_n \cong c_{n-1}$.

We start with the results on sandpile structures obtained via three-dimensional simulations [10]. Fig. 2 shows the variation of the steady-state volume fraction, ϕ , with the intensity of vibration ϵ . For $\epsilon > 1.0$ the volume fraction is only weakly dependent on ϵ with $\phi \cong 0.550 \pm 0.003$. However ϕ rises sharply as ϵ is reduced below $\epsilon = 1.0$ and, for $\epsilon \leq 0.2$, the shaken assembly adopts configurations which are more compact than those for sequentially deposited spheres. This is a clear manifestation of the collective nature of the structures which are introduced by a shaking process.

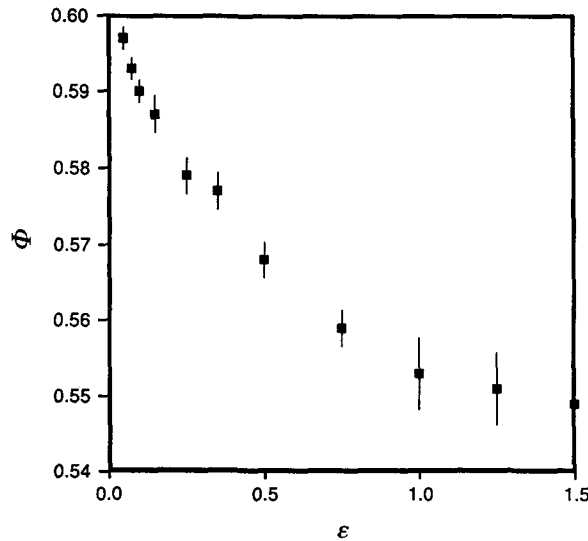


Fig. 2. The steady state volume fraction Φ of monodisperse hard spheres plotted against the shaking intensity ϵ .

Fig. 3 shows the variation of the steady-state mean coordination number of the spheres, c , with the intensity of vibration ε . For $\varepsilon \leq 0.25$ the mean coordination decreases as ε increases and it is approximately constant at $c \cong 4.48 \pm 0.03$ for larger intensities. The mean coordination number in a shaken assembly is substantially below that for a sequential deposit ($c \cong 6.0$) reflecting the presence of bridges and other void-generating structures. Also shown in fig. 3 are the mean fractions, $P(n)$, for $n = 3, 4, 5, 6$, of spheres which are n -fold coordinated in packings subjected to steady-state shaking vibrations at intensities $\varepsilon = 0.05$ and $\varepsilon = 0.5$. Most spheres touch four or five of their neighbours. For larger values of ε the proportion of four-fold coordinated spheres is increased, largely at the expense of six-fold coordinated spheres, i.e. the peak of the distribution moves towards lower coordination numbers.

From figs. 2 and 3 we note that for $0.25 \leq \varepsilon \leq 1.0$ the steady-state volume fraction steadily decreases with ε while the mean coordination number remains constant. This is consistent with the interpretation that, on the one hand, the density of bridges is independent of ε but that, on the other, the shapes of the bridges become in general more eccentric (and therefore more wasteful of space) as ε is increased.

Each stable configuration of spheres has associated with it a network, called

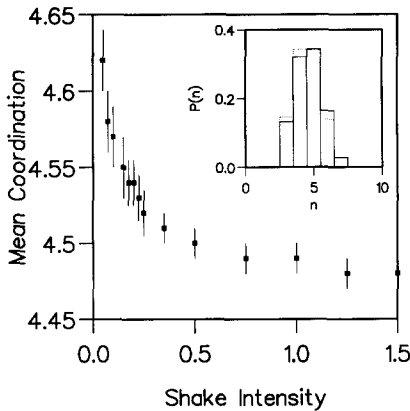


Fig. 3.

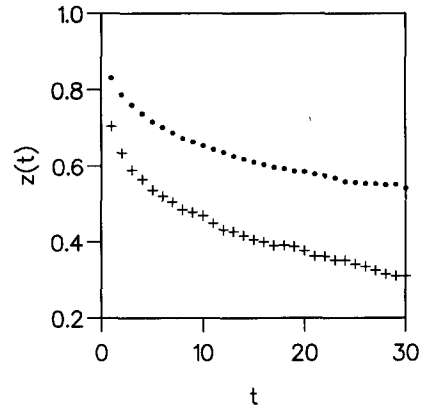


Fig. 4.

Fig. 3. The mean coordination number of monodisperse hard spheres plotted against the shaking intensity. The inset shows the mean fractions, $P(n)$, of spheres which are n -fold coordinated in the steady-state regime of the shaking process, which has shaking intensity $\varepsilon = 0.05$ (full lines) and $\varepsilon = 0.5$ (broken lines).

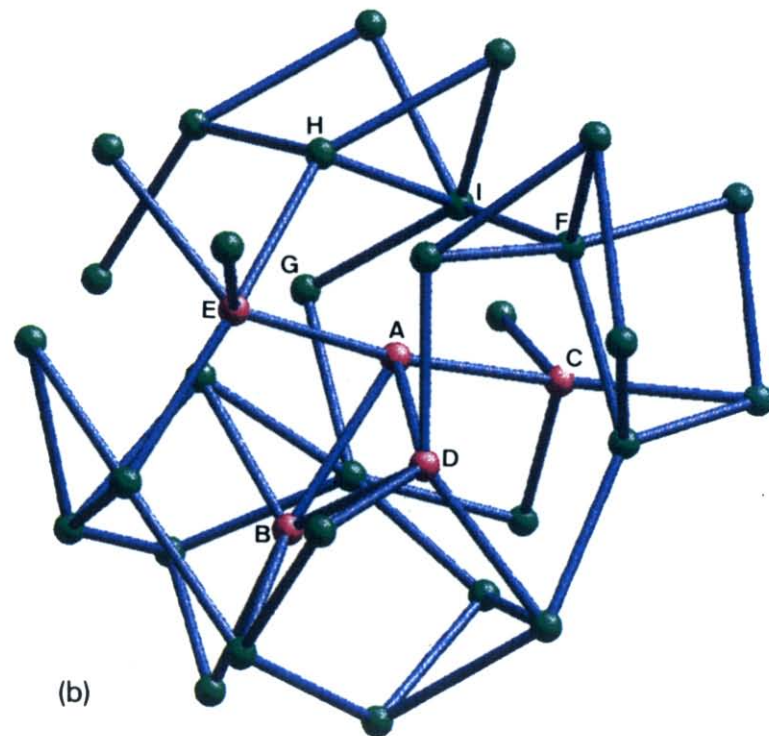
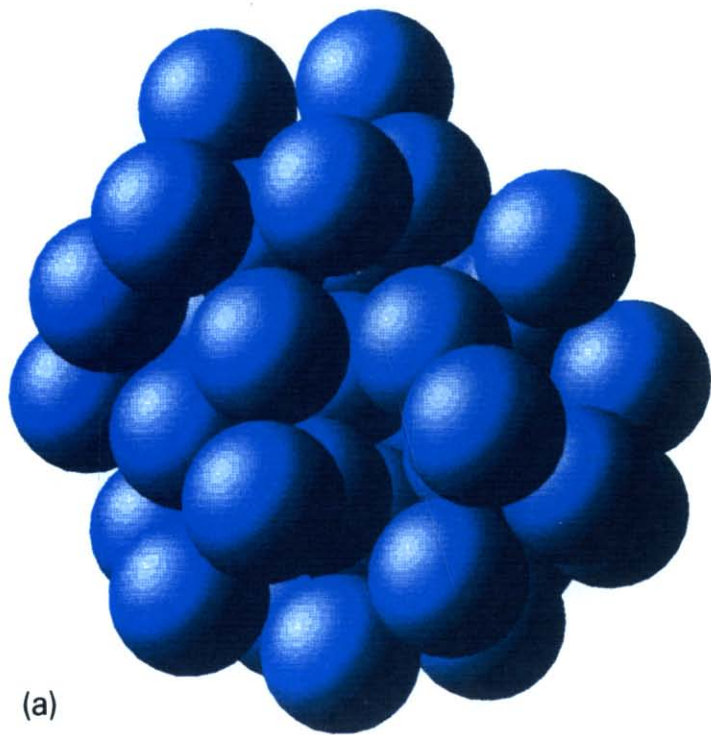
Fig. 4. The autocorrelation function, $z(t)$, of the contact network plotted against the number of shake cycles, t , for monodisperse hard spheres in the steady-state regime. The shaking intensities are $\varepsilon = 0.05$ (●) and $\varepsilon = 0.5$ (+).

the contact network, which can be formed by drawing line segments between the centres of all pairs of touching spheres. We have studied the evolution of the contact network in order to follow local sphere correlations during shaking. For each sphere i at time t we define an $(N - 1)$ -dimensional vector, $\mathbf{b}_i(t)$, such that the j th element of $\mathbf{b}_i(t)$ is unity if sphere i is touching sphere j , at time t , and zero otherwise. Fig. 4 shows the variation with time of the average autocorrelation function $z(t) = \langle \mathbf{b}_i(t') \cdot \mathbf{b}_i(t + t') / |\mathbf{b}_i(t')| |\mathbf{b}_i(t + t')| \rangle$, for spheres in the interior of the packing, at two shaking intensities $\varepsilon = 0.05$ and $\varepsilon = 0.5$. In both instances the initial rate of breaking of contacts is greatest and for larger times, $t \geq 10$, the rate becomes approximately constant. The main conclusion from the figure is that contact correlations disappear relatively slowly for low intensities of vibration: more quantitatively, we find that a single non-sequential reorganization with $\varepsilon = 0.5$ is approximately twice as efficient at disrupting the contact network as one with $\varepsilon = 0.05$.

The behaviour of $z(t)$ is consistent with snapshot observations of consecutive contact network configurations. Fig. 5 highlights the responses of a small group of neighbouring spheres, which are in the interior of a much larger packing, to vibrations of two different intensities. Fig. 5a shows the spheres which are instantaneously within a spherical capture volume and fig. 5b shows the contacts between them. We note that contacts between spheres at the periphery of the capture volume and spheres which are outside it are not represented in fig. 5. The capture volume is centred on sphere A and has a radius of approximately two sphere diameters. In figs. 5b–d small balls mark the positions of centres of the close-packed spheres and rods represent the sphere contacts. The initial configuration of packed spheres, which is a configuration obtained at the end of one particular shake cycle in the steady-state shaking regime with $\varepsilon = 0.05$, is shown in fig. 5a and its associated contact network is shown in fig. 5b. Figs. 5c and 5d are the contact networks for configurations which are obtained after the application of one further complete shake cycle, with intensity $\varepsilon = 0.05$ and $\varepsilon = 0.5$, respectively.

In the initial configuration sphere A rests on spheres B, C and D and is touched by one other sphere, labelled E, which rests on it. After an additional shake cycle with $\varepsilon = 0.05$ the sphere A remains stabilised in the same way but has gained a further contact, with sphere F, from above. There are many differences between the networks in figs. 5b and 5c but they are mainly small changes, of the sphere positions and rod orientations, which do not grossly alter the network connectivity. During the extra shake cycle, one sphere has left the capture volume and another has entered it so that the numbers of centres in figs. 5b and 5c are identical. The overall impression is one of network deformation.

In contrast, the network in fig. 5d does not closely resemble the one in fig.



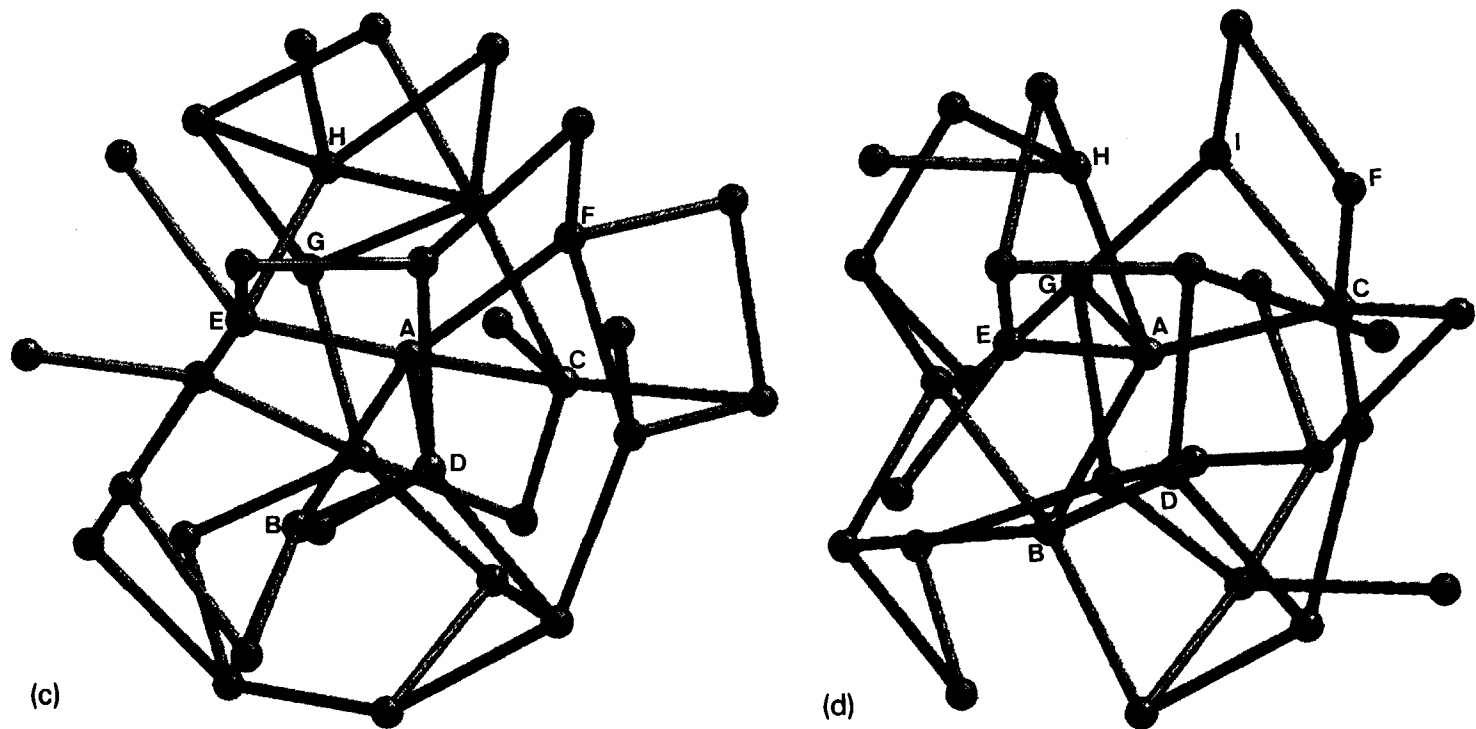


Fig. 5. (a) A three-dimensional representation of a cluster of 35 spheres. The cluster is part of a large assembly of spheres which has been subjected to shaking vibrations with intensity $\epsilon = 0.05$. (b) The contact network which corresponds to the cluster of spheres shown in fig. (a). Small balls represent the centres of the packed spheres and rods represent the contacts between them. The centres of the spheres B, C, D, E, which contact the central sphere A, have been coloured red. Contacts with the spheres that are outside of the cluster have not been shown. (c) The contact network which corresponds to the cluster of spheres which is obtained after the cluster in (a) is subjected to a further shake cycle with intensity $\epsilon = 0.05$. (d) The contact network which corresponds to the cluster of spheres which is obtained after the cluster in (a) is subjected to a shake cycle with intensity $\epsilon = 0.5$.

5b. There is a net loss of two spheres from the capture volume during the additional shake cycle with $\varepsilon = 0.5$. After this extra shake sphere A retains only two of its original supporting neighbours and gains a new one, sphere G. In this case the overall impression is one of network disruption. The network connectivity is altered significantly in this case, and a comparison of Figs. 5b and 5d shows many examples of bond creation and annihilation.

A notable insight to be gained from figs. 5b–d is that bridge collapse occurs more frequently for large vibrations. In fig. 5b, spheres H and I rest on, and support, each other and therefore form part of a bridge: this feature is retained in fig. 5c (contact network after small vibrations), but not in fig. 5d (contact network after large vibrations), where sphere H gains additional support by contacting sphere A from above. We see from a comparison of figs. 5b and 5d, that the bridge incorporating spheres H and I has collapsed after a single (large-intensity) shake.

We now consider the pair distribution functions of particle positions, $h(r)$ for separations in a horizontal plane and $g(z)$ for separations in the vertical direction. These are illustrated in fig. 6 for $\varepsilon = 0.05$ and $\varepsilon = 0.5$. In both directions the structure is similar to that expected for dense, hard sphere fluids. The short-range order is most pronounced in the horizontal direction, while the pair distribution function in the z -direction, $g(z)$, is relatively insensitive to variations of the shaking intensity. Both functions indicate the presence of a second shell of neighbours at a separation of approximately two particle diameters: we conclude from these figures that the short-range order decreases with increasing intensity of vibration, in accord with intuition.

During a shake cycle each particle, i , is shifted in position by $\Delta \mathbf{r}_i = \Delta x_i \mathbf{i} + \Delta y_i \mathbf{j} + \Delta z_i \mathbf{k}$ where $\mathbf{i}, \mathbf{j}, \mathbf{k}$ are unit vectors in the x -, y - and z -directions.

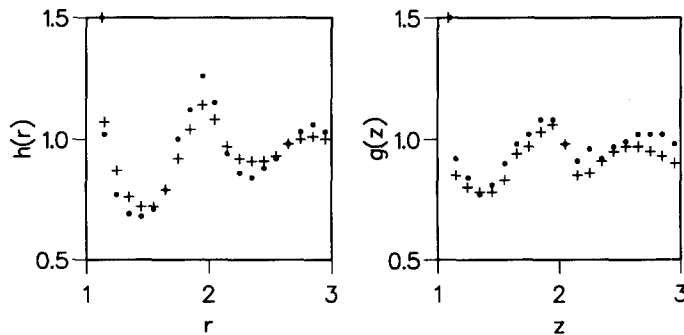


Fig. 6. The pair distribution functions of particle positions, $h(r)$ and $g(z)$, for monodisperse hard spheres in the steady-state regime, plotted against horizontal displacement, r , and vertical displacement z . The shaking intensity is $\varepsilon = 0.05$ (●) and $\varepsilon = 0.5$ (+). The peak heights, which are not shown, have been estimated as $h(1) = 6.35$ (6.30) and $g(1) = 4.40$ (4.25) for $\varepsilon = 0.05$ (0.5).

We have plotted, in fig. 7, correlation functions of the vertical components of displacement, Δz_i , for $\varepsilon = 0.05$ and $\varepsilon = 0.5$. $H(r)$ measures the correlations in a horizontal plane and $G(z)$ measures the correlations in the vertical direction according to

$$H(r) = \langle \Delta z_i \Delta z_j \delta(|t_{ij}| - r) \Theta(|z_{ij}| - \tfrac{1}{2}) \rangle / \langle |\Delta z_i| \rangle^2,$$

$$G(z) = \langle \Delta z_i \Delta z_j \delta(|z_{ij}| - z) \Theta(|t_{ij}| - \tfrac{1}{2}) \rangle / \langle |\Delta z_i| \rangle^2,$$

where $t_{ij}^2 = (x_i - x_j)^2 + (y_i - y_j)^2$, $z_{ij} = z_i - z_j$ and $\Theta(x)$ is the complement of the Heaviside step function. The averages are taken over all pairs of spheres i and j and over $m \cong 25$ shake cycles. We note that, over the range of shaking intensities we have studied, the mean size of vertical displacements during a shake cycle, $\langle |\Delta z_i| \rangle$, is a monotonic, increasing function of the intensity. Fig. 7a shows that $H(r)$ decreases rapidly to zero with increasing r and that there is a small decrease in the magnitude of the longitudinal displacement correlations, measured in the transverse direction, as the shaking intensity is increased. The data in fig. 7a give an estimate for the horizontal range over which the spheres move collectively during a shake cycle and thus provide a measure of the typical “cluster size” in the transverse direction.

Clearly, during vertical shaking, the motion of a particle is more sensitive to the positions and the motion of those neighbours which are above or below than it is to those which are alongside. Fig. 7b shows that the correlations of the longitudinal displacements measured in the longitudinal direction are stronger than those measured in the transverse direction, that is, $G(z)$ has a large first peak and, at large displacements, it decreases more slowly than $H(r)$. Also $G(z)$ depends strongly on the intensity of the vibrations and, for small ε ,

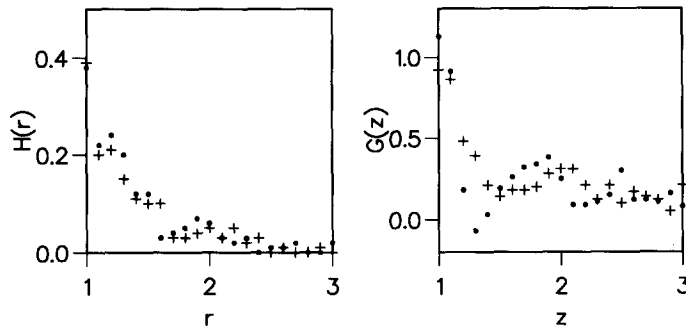


Fig. 7. The correlation functions, $H(r)$ and $G(z)$, for the vertical displacements of spheres during a single cycle of the steady-state shaking process, plotted against horizontal displacement, r , and vertical displacement, z . The shaking intensity is $\varepsilon = 0.05$ (●) and $\varepsilon = 0.5$ (+).

it has a distinct (negative) minimum at approximately $z = 1.3$ sphere diameters. This implies that at these separations, which are typical of vertical particle separations in shallow bridges, many sphere displacements are not strongly correlated, and several of them are moving in opposite directions: hence this feature is consistent with the slow compression or collapse of shallow bridges. The correlation functions of the transverse components of the sphere displacements are negative at small separations which is consistent with spheres sliding past each other as they are displaced in the x - and y -directions.

We conclude from all the above that the size of a typical dynamical cluster, in both longitudinal and transverse directions, decreases with increasing intensity of vibration. This verifies the predictions of the microscopic model [3], which says that collective (independent-particle) motions predominate for lower (higher) intensities of vibration.

In addition to furnishing data on the bulk properties our simulations can be used to obtain information about the surface of shaken particulate assemblies. Surface measurements are subject to larger uncertainties than bulk measurements because they involve only a fraction of the particles contained in the simulation cell and, also, because they are generally more susceptible to system size dependence. For simulations with $L = 8$ particle diameters and $N \cong 1300$ we have measured the mean square surface width, $\sigma^2 = L^{-2} \sum_i (z_i - z_0)^2$, defined by the spheres, i , which have heights z_i , and which are the highest spheres in each of L^2 vertical columns that have cross-sections of one square sphere diameter. Here z_0 is the mean height of the bed. All the surfaces that we have examined are smoother than the surface of a sequentially deposited aggregate which has $\sigma^2 = 0.44 \pm 0.02$. For $\varepsilon \leq 0.5$ the surface width is approximately independent of ε and $\sigma^2 \cong 0.16 \pm 0.02$. For larger shaking intensity σ^2 increases with ε and for $\varepsilon = 1.5$, $\sigma^2 \cong 0.23 \pm 0.02$. This is in keeping with the qualitative predictions [2] of our model, which states that greater surface roughening arises as a consequence of violent vibrations. We have not been able to establish the scaling properties of σ^2 ; however, we have confirmed that these trends are followed by other measures of the surface irregularity. Most notably we have used a Monte Carlo method to investigate the reaction surface for ballistic aggregation with small test particles, which have a diameter of 0.001 sphere diameters – in this case as well, the mean square width of the reaction surface follows the behaviour outlined above.

Other studies of surface roughening [39–41] have concentrated on the scaling regime appropriate to sequential deposition, in the presence of noise. Since our current approach is restricted to sizes below the scaling regime (because we incorporate complex and non-sequential reorganization processes), we are unable to compare our results on surfaces with those presented in refs. [39–41]. However, the results we have presented in ref. [10] are the *first* quantification

of surface roughening in cooperatively restructured packings. We hope to report further on the surface properties of shaken particulate assemblies, as well as the surface penetration effects, at a later stage.

We conclude the presentation of our computational results with a brief review of the results on slope relaxation obtained via a simulation in two dimensions [6]. In these we monitored the evolution of the pile over four decades of vibration cycles. Qualitatively similar results were obtained for two different geometries and for heaps of varying size. We saw [6] a clear logarithmic dependence of the slope on the time for large-intensity vibrations in qualitative agreement with the experimental data of Jaeger et al. [11], while for large times in the low-intensity case, we observed a “rounding off” of the top of our pile. Also, for the smaller vibrations, the contact correlations decreased slowly, at an approximately constant rate, while for the largest amplitude of vibration, the correlations decreased much more rapidly over short times [6]. This behaviour is consistent with the predictions of our microscopic model [2].

3.2.3. *Discussion of our results*

The computer simulation results we have presented establish links between the observed changes of the material properties, which occur as the shaking intensity varies, and the underlying microscopic correlations of the particle positions and displacements. From these results we identify competing roles for the independent-particle and the collective relaxation mechanisms which occur in non-sequentially reorganized random close packings – and verify earlier predictions [2] that independent-particle (collective) effects dominate at high (low) vibration intensity. Contact network measurements show that at high intensities individual particles are regularly ejected out of their local environments and, hence, one particle may sample many different environments over a short period of time. In contrast, at low shaking intensities, each particle experiences a slow deformation of its environment during shaking, and the identity of the particles which form its close neighbours remains relatively constant; thus, at these lower shaking intensities it is rare for a particle to make a transition into a totally new environment.

In our packings the particles which form parts of cooperative structures, such as bridges and arches, are subject to the different rates of change of their local environment caused by different shaking intensities. This leads to non-sequential reorganisation behaviour which depends, qualitatively, on the shaking intensity. During high intensity shaking, cooperative structures form and disappear rapidly so that most of the bridges, etc., which are present in one particular configuration are only one or two generations old. These

“immature” bridges have shapes which are those most favoured at their formation and these are, in general, wasteful of space. Thus the packing fraction takes a low value. In the low-intensity regime, the cooperative structures form and then deform, along with their local environment, over several further cycles before they become too tenuous to survive. In this case a packing may contain bridges which are many generations old (“mature”) and which have shapes that are favoured by their stability against disruption. This includes shapes which have relaxed downwards and are therefore “flatter”; the result is a higher packing fraction, i.e., a minimization of the void space, and a shift of the hole size distribution to smaller sizes.

According to our definition of a “bridge”, several of the spheres which form part of the structure will have a deficit of neighbours, particularly in the downward direction, and, therefore will have low coordination numbers. Thus the mean coordination number of a packing will depend on the density of bridge contacts and, in turn, this density will depend on the number density of the bridges and on the mean size of a bridge (i.e., the mean number of spheres which are required to construct one bridge). We can determine the latter from our measurements of $H(r)$; these indicate the lateral extent over which the vertical displacements of the spheres are positively correlated during one shake cycle and our results show (fig. 5) that the mean bridge width is quite insensitive to the shaking intensity. Non-zero correlations extend over approximately 1.5 sphere diameters indicating an average bridge width in the region of 3.0 sphere diameters, for both large and small intensities of vibration.

Given the observed independence of the mean coordination number on ε , for $\varepsilon \geq 0.25$, we infer that the number density of bridges is approximately constant in this regime. For $\varepsilon < 0.25$, the mean coordination number rises, which indicates (since the bridge size stays approximately constant) that the mean number density of bridges *falls*.

We now show the effect of the nature of the collapsed bridges on the resultant packing. For the lowest shaking intensities, the packing includes regions which result from slowly collapsed, “mature”, and flatter bridges, i.e. bridges which deformed considerably before their contact network was disrupted. We suggest that these are regions of particularly efficient random close packing and therefore cause the mean volume fraction to rise above the value which can be obtained by sequential packing processes. The enhanced short range correlations of the particle positions (cf. fig. 4), which we observed for $\varepsilon = 0.05$, are consistent with this interpretation. In the high-intensity regime, it is the “immature” and angular bridges which collapse, and the aftermath of such collapses is not distinguishable from a sequentially deposited structure, with smaller short-range correlations in particle positions and lower packing fractions. The above thus illustrates (via the specific mechanism of bridge

collapse) the point [2] that at low intensities of vibration, collective reorganisation of particles (and the consequent slow rearrangement of particle bridges) will lead to the efficient filling of voids, and the converse.

To conclude this subsection: we have presented a detailed study [6, 10] of the microscopic processes at work in the interior of a vibrated granular pile. In particular, we have presented a detailed study of the contact networks and their autocorrelation functions before and after vibration, and shown that earlier predictions [2] regarding the roles of independent-particle and collective relaxation mechanisms are verified. Finally, we have shown directly the dynamical behaviour of grains submitted to vibration, by examining the displacement correlation functions as a function of intensity, and demonstrating that the slow motion of clusters predominates at lower intensities, relative to the motion of independent particles, whereas the reverse holds for high intensities. The most promising future development in this area is experimental examination of our predictions – current experimental techniques using positron-emission tomography are an extremely powerful and novel tool for revealing the detailed dynamical behaviour of dry powders, and we expect to have substantial results [42] in this direction soon!

3.3. Theory – Langevin dynamics of sandpile relaxation

In this section we review recent theoretical work [9], based on a set of coupled Langevin equations to describe a sandpile relaxing under vibration.

Consider a pile of grains on a vibrating table. The state of the pile may be described by the macroscopic angle of tilt, θ , and ϕ , the local deviation from θ , caused by surface roughness, which is based on the definition of the Bagnold dilatancy angle [17]. The Bagnold angle, as originally defined, was the average extent to which clusters of particles protruded from the surface, which was in turn a measure [17] of the dilatancy [16]; we choose to work, instead, with $\Phi^2 \equiv \langle \phi^2 \rangle_{\text{pile}}$ and below will quantify Bagnold's idea by making an explicit connection between Φ^2 and the compactivity, X . As will be seen from fig. 8, small Φ corresponds to a well-packed pile (with low X) with a smooth surface, whereas large Φ corresponds to a loosely packed pile (with high X) with a rough surface.

It is well established [18] that any experimental measurement of the macroscopic angle of tilt θ lies between two limits, the so-called maximum angle of stability θ_m and the minimum angle of repose θ_r ; the difference between these two angles is Δ , the Bagnold angle, which, as has been pointed out by other authors [11], is a measure of the hysteresis. We make this idea more quantitative by interpreting Δ as the maximum value of Φ . In other words, Φ is a variable whose value is bounded by Δ , so that small values of Φ will lead to

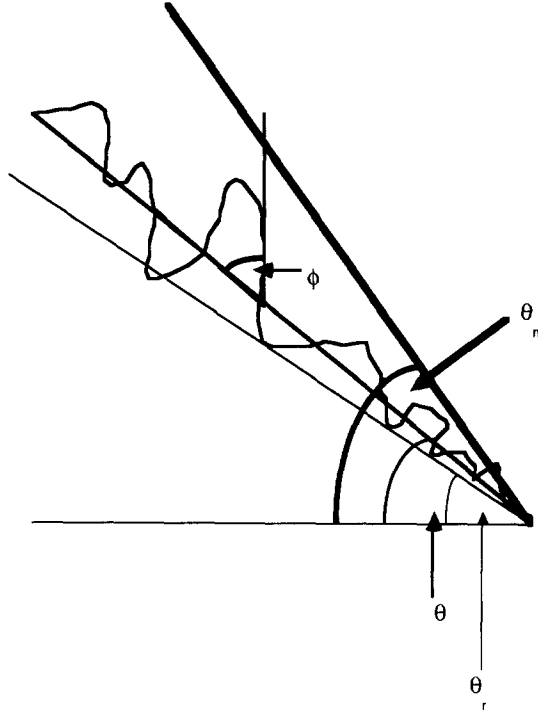


Fig. 8. The surface of a granular pile. The angles θ_r and θ_m are shown, corresponding respectively to the angles of repose and maximum stability; the measured angle θ varies between these two limits. The angle ϕ is the local deviation from θ .

measured angles θ nearer θ_r , while large values of Φ will lead to measured angles θ nearer θ_m . It is worth mentioning that the origin of Φ is dynamical, in that dynamics on the surface lead to disorder, which is the origin of hysteresis in the configurational properties of the pile [2, 9, 43].

In the presence of an applied vibration of intensity H (scaled by the gravitational acceleration) [2], θ and Φ will be time-dependent. The rate of change of θ is predominantly governed by independent-particle avalanches [2, 9]; therefore we view θ as representing the motion of independent particles. Conversely, if H is small relative to the binding energies of the particles, they are not ejected: in this case the grains reorganise within a cluster, i.e. they reorganise collectively to minimise voids. Since a finite value of Φ is a reflection of the presence of dilatant clusters on the surface, it is natural [2, 9] to associate the collective motion of these clusters with $d\Phi/dt$.

Although we have interpreted $d\theta/dt$ and $d\Phi/dt$ as though the corresponding relaxation processes were independent, we expect them to be coupled. Physically this coupling arises because a large roughness (large Φ^2) will increase the

value of θ as explained above, and a steeper slope (large θ) will sustain less roughness (small Φ^2). In keeping with the above discussion we write down coupled Langevin equations for θ and Φ :

$$d\theta/dt = -\gamma\theta - c\Phi^2 + \zeta(t) , \quad (4)$$

$$d\Phi/dt = -\Gamma\Phi - c'\theta\Phi + \xi(t) , \quad (5)$$

where γ and Γ are the rates controlling the θ and Φ relaxation processes, and c , c' are respectively the coupling constants relating the independent-particle and collective processes. The second term on the rhs of eq. (4) represents the contribution to $d\theta/dt$ (to lowest order) of the roughness: this can be viewed as representative of the average mismatch between the dilatancies of neighbouring clusters. The sign of this coupling is argued to be negative, as large mismatches (associated with large roughness) will enhance the value of θ , as discussed above, leading to an increase in the rate of decay of the slope. Correspondingly, the second term on the rhs of eq. (5) is bilinear in θ and Φ , and has a negative sign because large values of θ contribute to a decay of Φ , since steeper slopes can sustain less roughness. It is evident from eqs. (4) and (5) that the coupling term in the equivalent Landau–Ginzburg formulation of this problem is proportional to $\theta\Phi^2$. The respective noise terms ζ and ξ have the usual spectral properties

$$\langle \zeta(t) \zeta(t') \rangle = 2\langle \theta^2 \rangle_{\text{eq}} \gamma \delta(t - t') , \quad \langle \theta^2 \rangle_{\text{eq}} \propto H , \quad (6a)$$

$$\langle \xi(t) \xi(t') \rangle = 2\langle \Phi^2 \rangle_{\text{eq}} \Gamma \delta(t - t') , \quad \langle \Phi^2 \rangle_{\text{eq}} \propto X , \quad (6b)$$

where the subscript “eq” refers to the long-time limit in the presence of vibration. Eqs. (6a, b) are the fluctuation–dissipation relations for a driven granular system, with effective temperatures proportional to H and X respectively (throughout we take the constants of proportionality to be unity). Eq. (6a) ties in with earlier work [2, 5, 6, 10] as well as with the concept of granular temperature [1, 44]; in eq. (6b) we have made the reasonable assumption that the effective temperature associated with the relaxation of clusters is related to the density of packing, so that, for instance, clusters are able to rearrange more freely in loosely packed piles.

Let us now discuss the physical significance of the rate of independent-particle relaxation γ : we expect this to be governed by an activated process over a random distribution of barrier heights U related [2] to the configurational properties of a cluster. A suitable approximation is

$$\gamma(U) = \gamma_0 \exp(-U/H) . \quad (7)$$

Note that the effective temperature controlling these kinetics comes out naturally from eq. (6a). Γ , the rate of collective relaxation, is expected to be a similar function of the compactivity X ; however, for simplicity we consider Γ to be a parameter, not a distribution over energies.

We now present the full solution [9] of eqs. (1) and (2) in the presence of coupling. The relaxation time of a cluster is much larger than that of a particle (i.e. $1/\Gamma \sim N/\gamma$, where N is the number of grains in a cluster) so that the collective motion of the cluster, represented by Φ , forms a slowly evolving dynamical “cage” for the motions of the individual grains; consequently we use a mode-decoupling scheme for the “slow” variable Φ .

The final solution is [9]

$$\theta_{av}(t) = \exp[-\alpha(U)t] [A(U) I_\nu(\beta \exp(-\Gamma t)) + B(U) K_\nu(\beta \exp(-\Gamma t))], \quad (8)$$

where $I_\nu(x)$ and $K_\nu(x)$ are the modified Bessel functions, and

$$\alpha(U) = \Gamma + \frac{1}{2}\gamma(U),$$

$$\beta^2 \Gamma^2 = 2cc'[\Phi^2(0) - X],$$

$$\Gamma\nu(U) = +\{[\Gamma - \frac{1}{2}\gamma(U)]^2 + 2cc'X\}^{1/2},$$

and the subscript “av” denotes the average over the noise terms. The coefficients $A(U)$ and $B(U)$ were obtained by using the initial values of θ_{av} and $d\theta_{av}/dt$, so that

$$B(U) = \frac{-c\Phi^2(0) + \theta_{av}(0) \{\alpha(U) - \gamma(U) + \beta\Gamma[I_{\nu+1}(\beta)/I_\nu(\beta)] + \nu\Gamma\}}{\beta\Gamma\{[K_\nu(\beta) I_{\nu+1}(\beta)/I_\nu(\beta)] + K_{\nu+1}(\beta)\}},$$

$$A(U) = [\theta_{av}(0) - B(U) K_\nu(\beta)]/I_\nu(\beta).$$

These equations represent the full analytical solution to the decoupled problem. However, we now need to integrate over U ; this was done numerically, and some representative plots are shown in fig. 9, which show the form of $\theta_{av}(t)$ for large and small values of H , the intensity of vibration. We now analyse the above results; note that $\gamma(U)$ is bounded by $\gamma_{\max} = \gamma_0$ and $\gamma_{\min} = \gamma_0 \exp(-U_0/H)$. The form of the solution when the intensity of vibration is large, i.e. γ_{\min} is much larger than the other rate parameters like Γ or $\sqrt{2cc'X}$, is illustrated in fig. 9b. Although the decay in this figure is not logarithmic over the whole range, its form for times t such that $\gamma_0^{-1} \ll t \sim \gamma_0^{-1} \exp(U_0/H)$ is logarithmic. When, on the other hand, H is lowered, γ_{\min} decreases; then,

although the decay of $\langle \theta_{av} \rangle_U$ starts off being logarithmic even for small intensities of vibration, there is a crossover in its behaviour leading to a decrease in the slope of the graph (fig. 9c) which persists for a considerable time before the eventual decay to zero.

Let us now interpret these findings in the context of the experimental results. In the experiments [11], the regime of large-intensity vibrations was characterised by an apparently logarithmic decay. In our theory, the solution for large H in a given region of time is logarithmic (fig. 9a), but the functional form for arbitrary times is more complex. In the large H regime (fig. 9b), the decay is predominantly independent-particle-like, and the “log” decay over a relatively large range of times is a signal of this. The regime of small intensities of vibration is more interesting: we interpret the initial decay as being due to independent particles (“log” decay) albeit with a slower rate. Soon, the collective motion of the clusters takes over, so that there are essentially no avalanches due to independent-particle motion; this occurs in the flat portion of the curve of fig. 9c, where there is almost no decrease of slope. These slow motions of the clusters, when continued over a long time, generate overburdens at the surface that are metastable (because H is small, there is insufficient energy for particles to be ejected); however, when the cumulative effect of these overburdens becomes mechanically unstable, the pile collapses. In this limit, we see a complicated mix of collective and independent-particle motion. In the experiments [11], flattening of the θ vs $\log t$ curve at long times for small-intensity vibrations was also seen, but it proved impossible to go far enough out in time to observe the final behaviour in the slow regime. It seems that our theory provides an excellent framework within which to interpret those experimental results, and suggests what one might see at longer times than those so far observed experimentally. Work is presently in progress to formulate a theory where the local variations of the independent and collective coordinates are incorporated, thus enabling us to probe the *microscopic* dynamics of the pile.

We now return to the subject of hysteresis: as mentioned in the introduction, this is a particular characteristic of granular materials. Our theory shows the effect of hysteresis in the pile, via a “memory kernel” [9]; since Γ is small, the effects of the initial roughness ($\Phi^2(0)$) and slope ($\theta_{av}(0)$) persist for a long time. In addition to the coefficients $A(U)$ and $B(U)$, the *arguments* of the modified Bessel functions in eq. (8) contain these quantities, thus showing their importance for the relaxation processes: it may readily be shown [9] that these effects are particularly significant for small intensities of vibration, when the coupling of the two processes is comparable to the intensity H of the driving force. This is in accord with physical intuition; for small intensities of vibration, the predominantly collective relaxation process leads to slow configurational

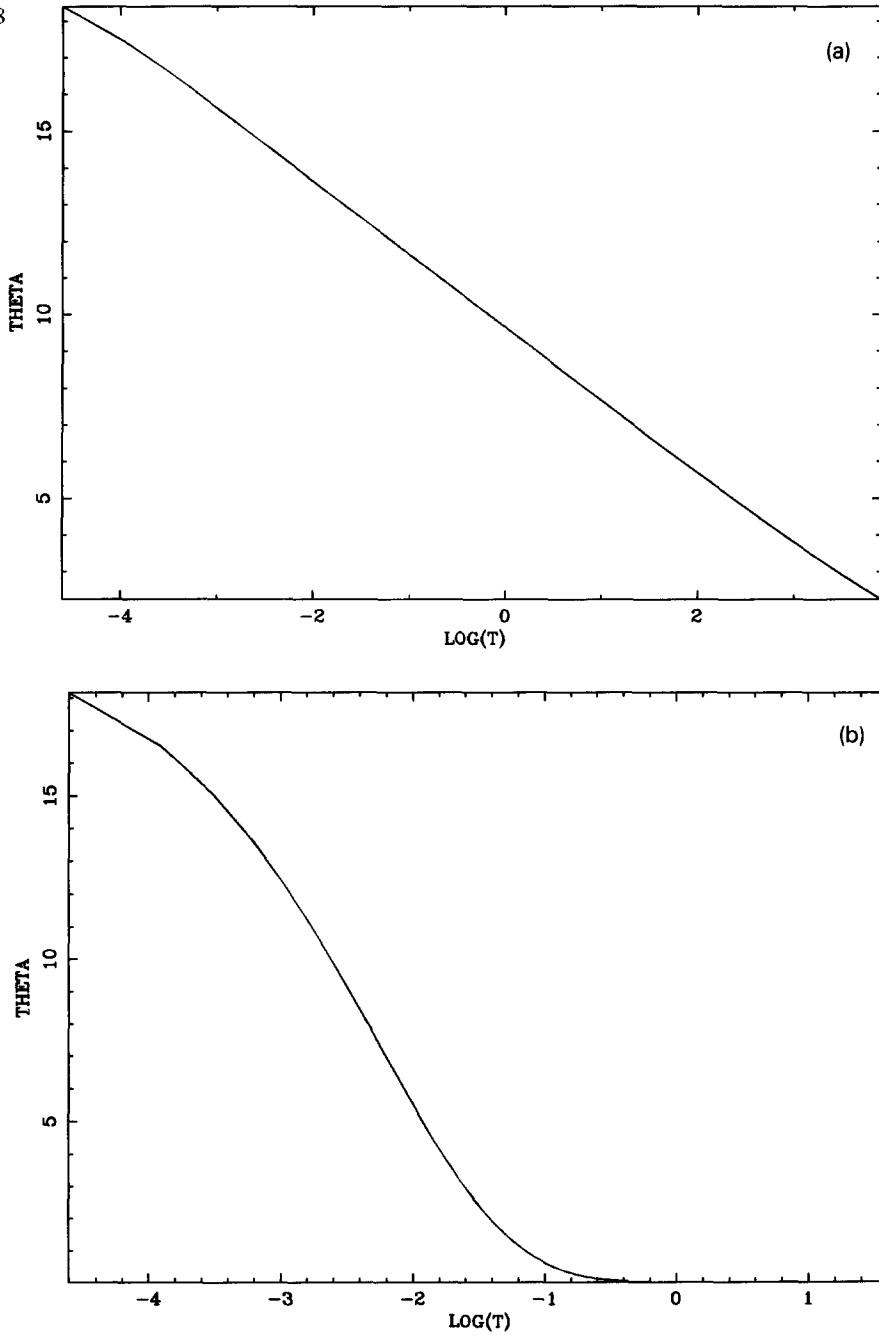


Fig. 9. θ_{av} versus $\log t$, with $\theta_{av}(0) = 20$ in each case: (a) In the absence of coupling, with $H = 10$. (b) For large H ($H = 10$) in the presence of coupling. The decay is rapid, and is logarithmic for the time scales specified in the text. (c) In the presence of coupling, for small H ($H = 0.1$). The initial decay is logarithmic until a crossover occurs, indicated by the flattening. Eventually, as predicted by eq. (9), θ_{av} drops to zero.

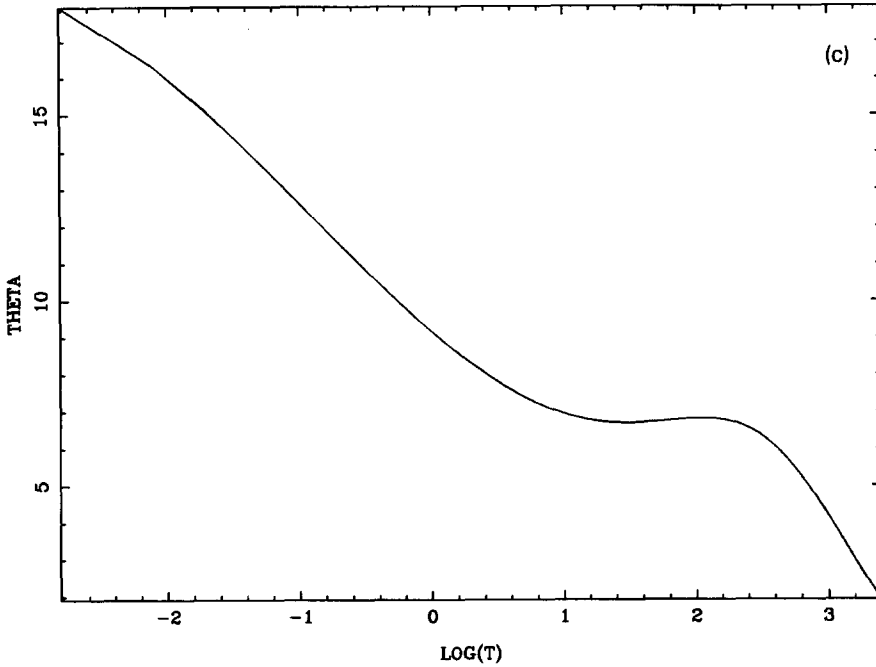


Fig. 9 (cont.).

changes, so that the memory of initial conditions persists for far longer times than is the case when H is large.

Since the dynamics of sandpiles is a new and active field in theoretical physics, it is perhaps worth emphasising some of the features that make our theory unique. We have defined coordinates for independent-particle and collective processes within the pile, and written down coupled Langevin equations for them. The preexisting concepts of H , the granular temperature [44] and X , the compactivity [3] have been unified within the framework of a consistent theory, which links each one to a dynamical variable via fluctuation-dissipation relationships. Our theory provides a quantitative illustration of two of the special features of powders, viz. dilatancy and hysteresis. The solution of the Langevin equations, obtained using a simple decoupling scheme, shows rich and complex behaviour, which is interpreted to arise from the competition and cooperation between independent-particle and collective relaxations. This solution, and our analysis of it, unifies earlier work [2, 5, 6, 10] and provides a reasonable basis for the interpretation of experiment [11].

4. Sandpiles in motion: is SOC relevant?

Recently Per Bak and his colleagues at Brookhaven proposed the theory of self-organised criticality (SOC), which states [23] that many large, multi-component and time-varying systems *organise themselves* into a special state, called the “critical” state. The claim was that the progress towards the self-organised state did not need the assistance of a driving force or an external influence but was somehow the result of the many-component nature of the system. The most striking and unusual feature of this special “self-organised” state is its invariance under rescalings of lengths and times; that is, no particular length or time scale stands out from any other.

To illustrate self-organised criticality, the Brookhaven group proposed a computer model of a “sandpile”. This toy “pile” is built from uniform square “grains” stacked on top of each other in columns. Grains are added to the pile, one at a time, onto the tops of the columns; the locations for the added grains are chosen at random so that the pile grows with an uneven surface. However, when the height difference between neighbouring columns reaches some pre-determined threshold, the surface grains flow, or fall, from the higher to the lower column. In turn, this movement may leave other neighbouring columns in an unstable conditions so that further surface flow could occur. The computer model completes all the surface movements, in a chain or “avalanche process”, before any further new grains are added.

If the computer simulation begins from a pile that already has a surface with a small slope, adding more grains causes the slope to increase until the angle of repose is reached. Further grains added to a pile in its critical state merely cause surface grains to slide off the pile leaving the slope unchanged. In the computer simulations, “sand” flows from the pile as single grains, as landslides covering the whole surface, and all possible cases in between, so that this preferred slope satisfies its description as critical. Furthermore, if one starts the simulation from a pile that is too steep, then adding grains causes a collapse until the slope is again at the same preferred value. In this way the model pile organises itself irrespective of the choice of starting condition. This toy sandpile is then an example of self-organised criticality.

It is now, however, widely recognised [7, 43, 46, 47] that real sandpiles do not conform to this blueprint. We consider first the experimental evidence: in experiments analysing the size distribution of avalanches, Sidney Nagel and his colleagues at the University of Chicago found that avalanches of one particular size, separated by regular intervals, dominated this flow. In an attempt to investigate this further, a research group at the IBM Research Centre in Yorktown Heights did controlled experiments [13] geared specifically to trace the flicker flow of sand from a pile. Their findings were as follows: for sandpiles

built on plates with diameters below one and a half inches, they detected a broad distribution of avalanche sizes, and a plot of weight against time showed similar fluctuations over one week to those over one hour. They claimed that this was clear evidence of self-organised criticality. By contrast, sandpiles built on three inch plates were dominated by avalanches where a large mass of sand was released: therefore self-organised criticality was *not* observed on larger piles. However, the work of the Chicago group disputes even this limited claim of purporting to observe SOC in smaller sandpiles: they argue [11, 46] that finite size effects dominate for the smaller sandpile, which cannot distinguish between the minimum angle of repose θ_r and the maximum angle of stability θ_m .

We turn now to theoretical evidence [43] against the existence of SOC in real sandpiles. Firstly, SOC is based on the idea of a single critical angle of repose, which is well known not to be valid for sandpiles [1, 18]. Secondly, theoretical studies of disordered cellular automata models [7] have shown that SOC cannot exist in the presence of (quenched) disorder; in ongoing work, we have improved on this by constructing cellular automata with annealed disorder [48] – we incorporate reorganisation of grains in surface layers which, because of friction between the grains, act as a memory bank for the pile. Therefore the disorder in the layers reflects all previous events, and as it anneals, has an effect on all subsequent events. Our preliminary results show clearly that with the addition of this realistic physics, sandpile automata *cannot* be characterised by SOC.

5. Conclusions

I hope I have infected the reader with at least part of my own passion and enthusiasm for sandpiles – I must stress that as this is a continuously evolving and very dynamic field, new developments are occurring as I write, so that any full stops in this article must be interpreted as points of suspension! For those of us lucky enough to have been in it at the start, it is precisely this whirlwind pace that gives it its buzz – and for my part, I'd like to welcome as many new members into our fold as possible to tackle the many outstanding, interesting, unsolved, and possibly unsolvable problems that challenge our curiosity.

Acknowledgements

I would like to thank the organisers of Statphys Calcutta for inviting me back to my home city, and for conducting an extraordinarily lively meeting – and the

audience for its interest in, and patience with, my five-hour lecture course! It is a great pleasure to thank all my collaborators in this work, who are (in alphabetical order of their first names) Gary Barker, Richard Needs, Sir Sam Edwards, Sushanta Dattagupta and Tom Duke.

Finally, I would like to thank Richard Needs and Mike Cates for their criticisms of this manuscript.

References

- [1] J. Bridgwater, *Powder Technol.* 15 (1976) 215; *Tribology in Particulate Technology*, M.J. Adams and B.J. Briscoe, eds. (Adam Hilger, Bristol 1987); R.M. Nedderman et al., *Chem. Eng. Sci.* 37 (1982) 1597.
- [2] A. Mehta, in: *Correlations and Connectivity*, H.E. Stanley and N. Ostrowsky, eds. (Kluwer, Dordrecht, 1990) pp. 88–108.
- [3] S.F. Edwards, in: *Proc. Enrico Fermi School of Physics*, Lerici (1988).
- [4] A. Mehta and S.F. Edwards, *Physica A* 157 (1989) 1091; S.F. Edwards and A. Mehta, *J. Phys. (Paris)* 50 (1989) 2489; A. Mehta and S.F. Edwards, in: *Disorder in Condensed Matter Physics*, J. Blackman and J. Tagüña, eds. (Oxford Univ. Press, Oxford, 1990).
- [5] A. Mehta and S.F. Edwards, *Physica A* 168 (1990) 714.
- [6] T.A.J. Duke, G.C. Barker and A. Mehta, *Europhys. Lett.* 13 (1990) 19.
- [7] J. Toner, *Phys. Rev. Lett.* 66 (1991) 679.
- [8] H.M. Jaeger, C. Lin, S.R. Nagel and T.A. Witten, *Europhys. Lett.* 11 (1990) 619; L.P. Kadanoff, S.R. Nagel, L. Wu and S. Zhou, *Phys. Rev. A* 39 (1989) 6524.
- [9] A. Mehta, R.J. Needs and S. Dattagupta, *J. Stat. Phys.* (1992), to appear.
- [10] A. Mehta and G.C. Barker, *Phys. Rev. Lett.* 67 (1991) 394; G.C. Barker and A. Mehta, *Phys. Rev. A* 45 (1992) 3435.
- [11] H.M. Jaeger, C. Liu and S.R. Nagel, *Phys. Rev. Lett.* 62 (1989) 394; C. Liu, H.M. Jaeger and S.R. Nagel, *Phys. Rev. A* 43 (1991) 7091.
- [12] G.W. Baxter et al., *Phys. Rev. Lett.* 62 (1989) 2825; G.W. Baxter and R.P. Behringer, *Phys. Rev. A* 42 (1990) 1017; *The Physics of Granular Materials*, A. Mehta, ed. (Springer, New York), in preparation.
- [13] G.A. Held et al., *Phys. Rev. Lett.* 65 (1990) 1120.
- [14] O. Zik, J. Stavans and Y. Rabin, *Europhys. Lett.* 17 (1992) 315; O. Zik and J. Stavans, *Self-diffusion in granular flows*, preprint.
- [15] C.-A. de Coulomb, in: *Memoires de Mathématiques et de Physique Présentées à l'Académie Royale des Sciences par divers Savants et Lus dans les Assemblées* (Paris 1773).
- [16] O. Reynolds, *Philos. Mag. Ser. 5*, 20 (1885) 469.
- [17] R.A. Bagnold, *Proc. R. Soc. London A* 225 (1954) 49; 295 (1966) 219.
- [18] R.L. Brown and J.C. Richards, *Principles of Powder Mechanics* (Pergamon Press, Oxford, 1966).
- [19] A. Mehta, *Rep. Prog. Phys.* (1992), to appear; *Chem. Eng. Science* (1992), review section, to appear.
- [20] A. Mehta, ed., *The Physics of Granular Materials* (Springer, New York), in preparation.
- [21] P.K. Haff, *J. Fluid Mech.* 134 (1983) 401; in: *The Physics of Granular Materials*, A. Mehta, ed. (Springer, New York), in preparation.
- [22] R. Jackson, in: *Theories of Dispersed Multiphase Flow*, R. Meyer, ed. (Academic Press, New York, 1983).
- [23] P. Bak, C. Tang and K. Wiesenfeld, *Phys. Rev. Lett.* 59 (1987) 381.

- [24] A.B. MacIsaac, N. Jan and A. Mehta (1992), in preparation.
- [25] P. Pusey, private communication; P. Bartlett and W. van Megen, in: *The physics of Granular Materials*, A. Mehta, ed. (Springer, New York), in preparation.
- [26] M.J. Vold, *J. Colloid Interface Sci.* 14 (1959) 158.
- [27] W.M. Visscher and M. Bolsterli, *Nature* 239 (1972) 504.
- [28] R. Jullien and P. Meakin, *Europhys. Lett.* 4 (1987) 1385.
- [29] T.A. Witten and L.M. Sander, *Phys. Rev. Lett.* 47 (1981) 1400.
- [30] A. Rosato et al., *Phys. Rev. Lett.* 58 (1987) 1038.
- [31] R. Soppe, *Powder Technol.* 62 (1990) 189.
- [32] C.S. Campbell and C.E. Brennan, *J. Fluid Mech.* 151 (1985) 167.
- [33] O.R. Walton, *Energy and Technology Review* (Lawrence Livermore Laboratory, May 1984).
- [34] P.A. Cundall and O.D.L. Strack, *Geotechnique* 29 (1979) 47.
- [35] G.C. Barker and M.J. Grimson, *J. Phys.: Condens. Matter* 1 (1990) 2779.
- [36] J.D. Bernal, *Proc. R. Soc. London A* 280 (1964) 299.
- [37] J.G. Berryman, *Phys. Rev. A* 27 (1983) 1053.
- [38] G.C. Barker, unpublished.
- [39] S.F. Edwards and D.R. Wilkinson, *Proc. R. Soc. London A* 381 (1982) 17.
- [40] M. Kardar, G. Parisi and Y.C. Zhang, *Phys. Rev. Lett.* 56 (1986) 889.
- [41] R. Jullien and R. Botet, *Phys. Rev. Lett.* 54 (1985) 2055.
- [42] T.D. Beynon, A. Mehta and J. Bridgwater, in preparation (1992).
- [43] A. Mehta and G.C. Barker, *New Scientist* (15 June 1991) 40.
- [44] P.-G. de Gennes, unpublished.
- [45] M. Abramovitz and I.A. Stegun, *Handbook of Mathematical Functions*, (Nat. Bur Stand., Washington, DC, 1964).
- [46] S.R. Nagel, *Rev. Mod. Phys.* 64 (1992) 321.
- [47] P. Bak and M. Creutz, *MRS Bull. XVI*, No. 6 (June 1991) 17.
- [48] A. Mehta and G.C. Barker, to be published.